Journal of The Electrochemical Society, **148** (4) H29-H36 (2001)
0013-4651/2001/148(4)/H29/8/$7.00 © The Electrochemical Society, Inc.

A pH Electrode Based on Melt-Oxidized Iridium Oxide

Sheng Yao,* Min Wang,* and Marc Madou[z]

NSF Center for Industrial Sensors and Measurements, The Ohio State University, Columbus, Ohio 43210, USA

Fabrication and characterization of a novel potentiometric pH electrode based on melt-oxidized iridium oxide film is presented. The oxide film produced in a lithium carbonate melt has the composition of $Li_xIrO_y \cdot nH_2O$, and shows high chemical stability. The electrode based on this oxide film exhibits very promising pH sensing performance, with an ideal Nernstian response in the tested pH range of 1 to 13. The potential response is fast, with a 90% response time obtained in less than 1 s for all pH changes. The open-circuit potential of the electrode is almost drift-free, with an average variation over time in a pH 6.6 solution as small as 0.1 mV/day. Furthermore, the potential/pH slopes and the apparent standard electrode potentials show excellent agreement among electrodes from the same batch. A comparison is made of the present electrode and those reported in the literature with respect to fabrication method and pH sensing characteristics.
 [DOI: 10.1149/1.1353582]

Manuscript submitted April 8, 1999; revised manuscript received December 5, 2000.

Glass pH electrodes have been widely used because of their good sensitivity, selectivity, stability and long lifetime.[1] However, glass electrodes have several disadvantages due to the intrinsic nature of the glass membrane. For example, glass electrodes are easily affected by alkaline or HF solutions, they require a high input impedance pH meter, they often exhibit a sluggish response, and are difficult to miniaturize and planarize based on current manufacturing technologies.[2] Moreover, these electrodes cannot be used in food or *in vivo* applications because of their brittle nature and the risk of leaving sharp bits of glass behind. Drawbacks of glass electrodes have led to intensive research for alternative pH electrodes. Potentiometric metal oxide electrodes have proven to be some of the most promising candidates.

Various solid-state metal oxides have been investigated for pH electrodes. Among them, the Sb_2O_3 electrode[3] is by far the most widely used, especially in acid-base titration or in solutions containing HF, although it is not suitable for accurate measurement of pH due to the drift of response potential. Einerhand *et al.*[4] introduced a Bi_2O_3 electrode to measure pH in a concentrated KOH solution, a medium in which the glass electrode cannot be used. Liu *et al.*[5] developed a PdO electrode for measuring the pH of whole blood. A Nafion film was coated on the electrode to prevent the PdO from dissolving into Cl^- contained solutions. Grubb *et al.*[6] demonstrated a PdO electrode with a long lifetime but suffering redox interference. Fog *et al.*[7] surveyed various metal oxides including PtO_2, IrO_2, RuO_2, OsO_2, Ta_2O_5, RhO_2, TiO_2, and SnO_2. The results on pH sensitivity, working pH range, ion and redox interferences, and hysteresis indicated that IrO_2 and RuO_2 held the most promise. RuO_2 electrodes exhibit a near Nernstian response in a wide pH range, but drifts for both of the potential/pH slope and the apparent standard electrode potential ($E°'$) were identified.[8,9]

Iridium oxide (IrO_x) electrodes have received considerable attention in recent years.[10-31] Their advantages over conventional glass electrodes and other metal oxide electrodes were shown to include good stability over a wide pH range, even at high temperatures up to 250°C,[24] at high pressure,[18] and in aggressive environments,[19,29] and show fast response even in nonaqueous solutions.[22,31] Besides its use as a pH electrode, IrO_x is also well known as an anode material for oxygen and chlorine evolution[32] and as an electrochromic material.[33] For all these applications, the characteristics of IrO_x are generally very sensitive to its structure and composition, which depend on the fabrication method and condition. This is the main reason that most of the IrO_x pH electrodes prepared by different methods show different characteristics. Some IrO_x pH electrodes reported in the literature are summarized in Table I. In the table the electrodes are classified according to the fabrication methods of the iridium oxide films (IROFs): mainly electrochemical growth, electrodeposition, reactive sputtering, and thermal preparation as detailed below.

A considerable amount of research has focused on the electrochemical growth of IROF.[10-14] In this method an IROF is grown on the surface of an Ir metal electrode by cycling the electrode potential repeatedly between the potentials corresponding to H_2 and O_2 evolution, typically -0.25 to 1.25 V *vs.* standard calomel electrode (SCE) in 0.5 M H_2SO_4. Under potential cycling conditions, *i.e.*, cyclic scans or pulses, a thick hydrous IrO_x film grows, which will not occur under any fixed potential condition.[33] It is interesting that, for sustained IROF growth to occur, the potential must exceed critical upper (E_g^+) and lower (E_g^-) potential limits during each cycle, which is not required for other metals such as Pt, Ru, Ni, Fe, etc. This type of IROF is known by the acronym AIROF (anodic iridium oxide film). AIROFs are poorly crystallized, mostly in amorphous phase and are highly hydrated, and can actually be regarded as a gel-like material.[34] As can be seen from Table I, AIROF based electrodes commonly exhibit unpredictable, often super-Nernstian slopes, mostly in the range from -60 to -80 mV/pH rather than the expected value of -59 mV/pH. This special feature is explained by the assumption that more than one proton is involved per electron in the potential determining reaction.[34] Table I also shows that the results reported by different authors for AIROF based electrodes are quite scattered, not only in $E°'$, but in the slopes as well. It has been accepted that this phenomenon results from differences in fabrication conditions which lead to differences in the oxidation state and the extent of hydration of AIROFs. Burke *et al.*[10] noticed that the variation of the potential/pH slopes is associated with the difference in the degree of hydration of the AIROF. Hitchman *et al.*[12] found that both the slopes and $E°'$ were strongly affected by an anodic pretreatment of the electrode. Along the same line, Olthuis *et al.*[13] correlated the slope with the oxidation state of the AIROF, and concluded that the higher the oxidation state, the higher the slope. It is also found that the pH sensing characteristics are somehow dependent on the crystal structure and even the thickness of AIROFs. Kinoshita *et al.*[11] compared mono- and polycrystalline AIROFs and found that the former was superior in pH response stability. Hitchman *et al.*[12] suggested that thicker AIROF should be able to ensure more reproducible pH response behavior. Unlike glass electrodes, metal oxide electrodes usually suffer redox interference due to the fact that metal oxides are mixed conductors and both electrons and ions may determine the potential.[2] Song *et al.*[14] investigated interference by oxy-sulfur anions and found that the interferences from redox-inactive species such as sulfate and sulfite were negligible, while those from reducing anions such as bisulfite and thiosulfate were so severe that the AIROF was reduced irreversibly.

* Electrochemical Society Student Member.
[z] E-mail: madou.1@osu.edu

Table I. Performance of iridium oxide-based pH electrodes made by different methods.

Method	Electrode	Sensitivity (mV/pH)	$E^{\circ\prime}$ (mV, *vs.* SHE)[a]	Total drift[b] (mV)	Authors/Year
Electrochemical growth (AIROF)	IrO_2/Ir Wire (0.5 mm diam)	77.7 (25°C)	1240	-[c]	Burke *et al.*[10] 1984
	IrO_2/Ir wire (0.6 mm diam)	71.2	714	-	Kinoshita, E. *et al.*[11] 1986
	IrO_2/Ir wire (1 mm diam)	75 (25°C)	925	35	Hitchman *et al.*[12] 1988
	IrO_2/Ir wire (0.15 mm diam)	62-74 (21°C)	734-1066	15-130	Olthuis *et al.*[13] 1990
	IrO_x/Ir wire (0.5 mm diam) (deeper purple tint)	74-78	909-934	-	Song *et al.*[14] 1998
Electrodeposition	(Pd-Ir)O_x/glassy carbon (3 mm diam)	62 (pH <6, 21°C) 83 (pH >6)	910 ± 6 (pH < 6) 1020 ± 20 (pH >6)	-	Jaworski *et al.*[15] 1992
	IrO_x/glassy carbon (1.5 mm diam) (bright blue)	63-82	940-1120	25	Baur *et al.*[16] 1998
	Nafion/IrO_2/Pt/Kaption film	61-65(22°C)	~810	-	Marzouk *et al.*[17] 1998
Sputtered coating (SIROF)	IrO_x/Ta or stainless steel (1500Å, dark blue)	59.5 (19°C) 68.8 (80°C)	1042	220	Katsube *et al.*[18] 1982
	IrOx/alumina (1500-7500Å)	55-60(22°C)	995 ± 35	200	Tarlov *et al.*[20] 1990
	IrO_2/sapphire sheet (1000Å, dark blue)	59 (25°C)	880	10	Kato *et al.*[21] 1991
	IrO_x/alumina or silicon wafer	54-49 (22°C)	1016	150-200	Kreider *et al.*[23] 1995
Thermal method	IrO_2/Ir wire (blue black)	62.8 (4°C)	930 ± 5	-	Papeschi *et al.*[25] 1976
	IrO_2/Ti ($IrCl_3$ decomposition)	59	950	-	Ardizzone *et al.*[26] 1981
	IrO_2/Ti ($IrCl_3$ decomposition)	59 (25°C)	982 (fresh)	80	Kinoshita, K. *et al.*[27] 1984
	IrO_x/Ir wire	59 (25°C)	1000-1172	200	Hitchman *et al.*[28] 1992
	(blue-black)	59 (25°C)	870 (after pretreatment)	10	
	Nafion/IrO_2/Ti $IrCl_3$ decomposition, blue-black)	51-56 (22°C)	850-856	-	Kinlen *et al.*[30] 1994
Printing method	IrO_2/inert matrix	59.8 (25°C)	~900	-	Fog *et al.*[7] 1984
Current method (Thermal method)	IrO_x/Ir wire (deep black)	58.9 (22°C)	923	0.2	Current paper

[a] Some data is calculated by assuming that Ag/AgCl reference electrode potential is 197 mV *vs.* SHE.
[b] Different papers report drift data over varying periods of time.
[c] (-) indicates that the data is unclear.

Electrodeposition of IROF based on electrolysis of a solution containing Ir complexes is less used.[15-17] In this method, IROF can be deposited on a variety of electronically conducting substrates, such as glassy carbon, Ti, Pt, or Pt/Kapton film. This method is useful to produce ultramicroelectrodes and is less expensive than the electrochemical growth method, since it does not require Ir substrates. However, preparation of the deposition solution is somewhat complicated and a freshly prepared solution is required for each deposition. Similar to AIROF, IrO_x made by this method is also hydrated and gives super-Nernstian slope as shown in Table I. Jaworski *et al.*[15] deposited an Ir-Pd oxide film on a glassy carbon electrode (GCE) from a Na_2IrCl_6-$PdCl_2$ solution. Baur *et al.*[16] recommended the same method, but used an iridium(III) oxide as the deposition solution. Marzouk *et al.*[17] produced a planar electrode by depositing an IROF on Pt sputtered Kapton film.

Sputtering deposition of IrO_x electrodes has become quite popular.[18-23] This method has the advantage that small planar electrodes, even microelectrode arrays can be patterned onto a small area on various substrates. Therefore, it is compatible with MEMS (microelectromechanical systems) fabrication techniques in general.[35] Compared with AIROF, sputtered iridium oxide film (SIROF) based electrodes can provide more reproducible potential/pH slope, which is Nernstian or near-Nernstian. However, other parameters, such as $E^{\circ\prime}$, drift, and redox interference, etc., are tightly related to the sputtering condition, such as oxygen partial pressure, argon pressure, humidity, deposition rate, substrate temperature, electric field, etc.[18,35] In addition, the sputtering technique is relatively costly because of the expensive Ir target, although various cheap substrates can be used. Katsube *et al.*[18] found that the $E^{\circ\prime}$ value was not sensitive to the substrate employed, but from the viewpoint of adherence, stainless steel and Ta are more effective. They attributed the potential drift to a slow hydration of the SIROF, which consequently causes a change of the oxidation state of the oxide film. Their results showed that metal cations lead to small interferences, while dissolved oxygen induces a large interference. Lauks *et al.*[19] identified the utility of an SIROF based electrode for measurements in concentrated HF. Tarlov *et al.*[20] deposited an SIROF in a water-saturated oxygen atmosphere to reduce the redox interference, but a large aging effect was observed with their electrodes. They mentioned that this process was not completely irreversible, *i.e.*, the $E^{\circ\prime}$ value of an aged electrode can be effectively reversed by exposing the electrode to air again. Kato *et al.*[21] employed a low deposition rate (5 Å/min) to prepare electrodes, good stability and less redox interferences were achieved. Furthermore, this electrode turned out to be useful to measure nonaqueous solutions.[22] Kreider *et al.*[23] compared several sputtered metal oxide electrodes including PtO_x, PdO_x, RuO_x, and IrO_x; significant drift and hysteresis were observed for all of these electrodes.

Several preparation approaches belong to the thermal deposition method.[24-31] The most popular one is based on pyrolysis of $IrCl_3$ on a Ti substrate at 400-500°C.[26,27,30] Other thermal methods include oxidation of Ir wire in a molten KNO_3 at 420°C,[24] or direct oxidation of Ir metal (previously wetted in a NaOH solution) in air at 800°C.[28] IrO_2 prepared from $IrCl_3$ was found to contain as high as 2 wt % of residual Cl^- which is difficult to eliminate.[36] Thermally prepared IROFs can be made much thicker than AIROFs, and provide more reliable potential values.[24] Generally, thermally prepared IrO_x films are comparable in nature to SIROF. Both are called ''dry'' oxide films (anhydrous films) as they are less hydrous than

AIROF, which is formed in an aqueous solution. Usually the wetting of the dry oxide films in water is a very slow process, which can take even more than 2 months.[32] Therefore, it is understandable that the dry film-based electrodes often exhibit large aging effects, usually with the potential moving in a negative direction. Most thermally oxidized IrO_x films exhibit a cracked, dried mud appearance.[26] Papeschi *et al.*[25] reported that this kind of IrO_x electrode was not sensitive to dissolved oxygen and stirring, and had a temperature coefficient of 1.27 mV/°C between 0 and 40°C. Kinoshita *et al.*[27] observed that the $E°'$ drifted negatively about 80 mV by aging the electrode in water for two weeks, but the slope remained unchanged. They proposed that this drift resulted from structural changes of the oxide by hydration. Hitchman *et al.*[28] introduced a slow potential sweep treatment to reduce the potential drift and to converge $E°$ values for different electrodes. Kinlen *et al.*[30] reduced the redox interference by coating a permselective membrane, which is permeable to cations but not anions, thus the interference from redox anions such as ferricyanide and ferrocyanide can be eliminated. Ue *et al.*[31] evaluated a thermally prepared electrode in a nonaqueous solution, *i.e.*, dimethyl sulfoxide, and found that it exhibited faster pH response than a glass electrode.

Many approaches such as optimizing the preparation conditions, using surface treatments or coating a membrane have been proposed and proved to be effective to improve the IrO_x electrode stability and selectivity as discussed above. However, the potential drift, which causes errors in pH measurement, remains a serious obstacle to the widespread application of IROF-based pH electrodes. From our own work, we learned that the potential drift phenomenon results from various factors, such as the oxidation state, the degree of hydration, etc. All of these factors are influenced by the preparation method of the oxide film. The oxidation state and hydration of the oxide film are important factors for long-term stability of the electrode. If the equilibrium between oxidation and/or hydration states is disturbed by environmental changes, a new equilibrium will be established, resulting in potential drift. The drift usually is a very slow process, but in some cases it can be as fast as 200 mV within a couple of hours for freshly prepared IrO_x electrodes.[13,18,20] To solve these problems, obviously, the key is to produce a high quality IROF.

Given this background we have developed a new approach to prepare IrO_x pH electrodes, *i.e.*, a high temperature oxidation method, in which an IROF is formed on an Ir metal wire in a carbonate melt. To the best of our knowledge, there is no report of using a carbonate melt to oxidize a metal for the purpose of fabricating a metal oxide film. The IrO_x electrode produced by this new method shows very promising pH sensing characteristics, and can serve as an attractive candidate for a future generation of pH sensors. In the present paper, the fabrication and pH sensing performance of the IrO_x electrode as well as the characterization of the oxide film are presented.

Experimental

Preparation of IROF and electrode.—Ir metal wires (0.127 or 0.25 mm in diam, 99.8% purity, obtained from Alfa AESAR) of about 10 mm in length were ultrasonically cleaned with 6 M HCl following with deionized water. The cleaned wires were positioned in a gold foil lined alumina crucible and covered with Li_2CO_3 powder (anhydrous, purity >99%, obtained from Alfa AESAR). Although several kinds of alkali carbonates have been used in the experiments, including Li_2CO_3, Na_2CO_3, and K_2CO_3, in the present paper, all results are based on Li_2CO_3. The oxidation of the Ir wires was performed at 870°C for 5 h in a furnace under air atmosphere. At this temperature, Li_2CO_3 is in its liquid state without significant decomposition for the duration of the experiment. After cooling down to room temperature, the solid carbonate in the crucible was dissolved by a HCl solution. And the oxidized wires were then washed with deionized water to remove any attached soluble components. Finally, the wires were dried at 120°C overnight. As a result, a thick, deep black, cohesive oxide layer grew on the surface of the wire. Within a batch, usually 10-20 oxidized wires were produced. In the present paper, the electrodes used come from two different batches, *i.e.*, batch I and batch II as addressed in each figure. To fabricate the pH electrode, a small area (about 1 mm in length) of the IROF at one end of the oxidized wire was scraped off, and a gold wire (0.1 or 0.25 mm in diam) was wound around this bare end to form a good physical and electrical connection. In some cases, the gold wire was thermally soldered onto the Ir wire. An organic adhesive was applied to cover the contact area and the connecting wire to provide electric insulation.

Characterization of the IROF.—The morphology of the obtained IROF was investigated using a Philips XL30 FEG scanning electron microscope (SEM). X-ray photoelectron spectroscopy (XPS) measurements were performed in a Vacuum Generators, ESCA LAB Mark IV, a spectrometer with separate sample preparation and secondary ion mass spectrometry (SIMS) chambers. Spectra were taken using Mg Kα as the radiation source with analyzer pass energy of 50 eV. The measured electron binding energies were charge corrected according to the C 1s peak at 284.6 eV. Before the study, the IrO_x sample and commercial IrO_2 powder as reference were dried at 120°C overnight. Elemental analysis was carried out using a Perkin-Elmer Optima 3000 inductively coupled plasma optical emission spectrometer (ICP-OES) and a Sciex Elan 6000 ICP mass spectrometer (ICP-MS). For elemental analysis, the IrO_x sample was scraped off from the surface of the oxidized wire, then dissolved by fusing with KOH melt. After cooling, the fused material was dissolved in a 10% H_2SO_4-5% HNO_3 (v/v) solution.

pH response.—Open-circuit potentials (OCPs) of IrO_x electrodes were measured as a function of the pH of the test solution against a single junction Ag/AgCl reference electrode (with 4 M KCl internal solution, obtained from Fisher Scientific) using a digital multimeter, a data acquisition/switch unit (HP34970A), and a computer (Gateway 2000). The software used in data collection is HP Benchlink Data Logger. The reproducibility of the IrO_x electrodes was evaluated by measuring a group of electrodes under identical conditions. Before measurement, IrO_x electrodes were stored either dry, or in a 4 M KCl solution. The temperature of the test solution was recorded by a thermistor. All potentiometric measurements were carried out at room temperature of 22 ± 3°C. To investigate the pH sensing characteristics, the pH change of the test solution was realized in two different ways.

In one method (method I), the measurement was carried out in a series of commercial pH buffer solutions from pH 1 to 13 (obtained from Fisher Scientific). In this case, the pH change was realized by switching the IrO_x electrode from one pH buffer solution to another. The buffer solutions are air-saturated without stirring. In this method, the pH values of the fresh commercial pH buffer solutions are exactly known, therefore a high accuracy of the calibration curve can be obtained without the need of calibration by a commercial glass electrode.

The other method (method II) for changing the pH of a test solution was based on an acid-base titration. The pH electrode was immersed into a base solution, which was added KOH or HCl to increase or decrease its pH to a desired value. A homemade universal pH buffer solution, composed of 0.1 M H_3PO_4-H_3BO_3-CH_3COOH and 0.1 M KCl, with an initial pH value near 2, was employed as the base solution. The pH range of this method was 2 to 12. A conventional three-neck Pyrex flask containing 150 mL of the base solution served as a measurement cell. The solution in the cell was magnetically stirred and air saturated but not thermostated. A previously calibrated glass electrode (from Orion) and a digital pH meter (Orion, model 720A) were used to monitor the pH of the solution.

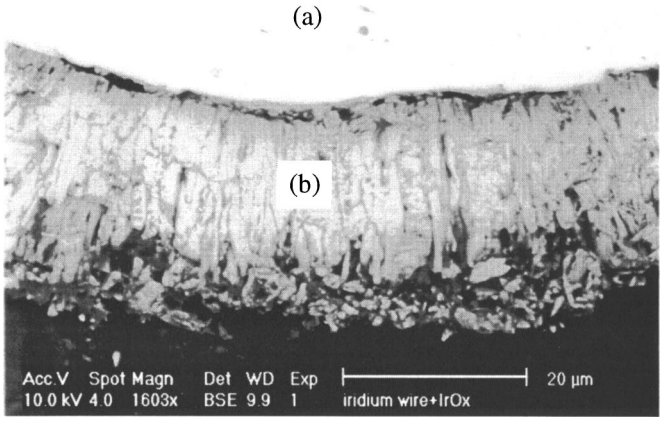

Figure 1. SEM image of the cross section of the IROF: (a) Ir wire with a diam of 0.25 mm, (b) IROF. The IrO_x grows from the Ir wire with a high aspect ratio columnar structure. The thickness of the IROF is about 20 μm.

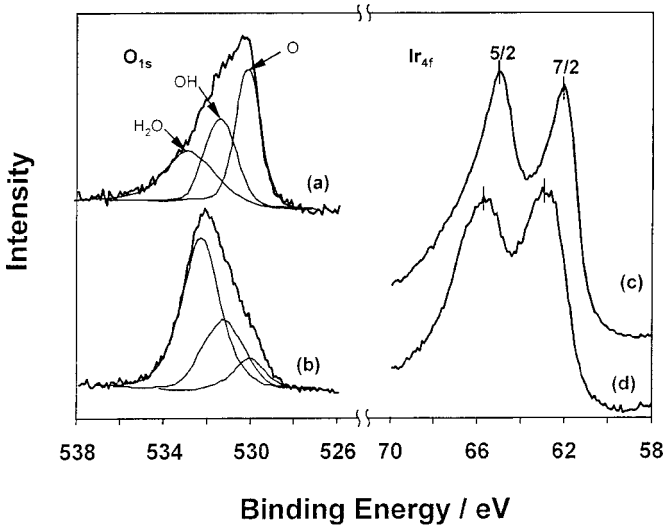

Figure 2. XPS spectra of (a), (c) O 1s and Ir $4f_{7/2,5/2}$ levels of commercial IrO_2 power and (b), (d) IrO_x powder. The peak decomposition of the O 1s peaks contributed from oxide, hydroxide, and water as presented.

Results and Discussion

Investigation of the IROF.—An investigation of the physical properties, including surface morphology, adhesion, solubility, and color of the IROFs, was performed. The observation of the oxidized wire in SEM shows that the IROF is very uniform. This can be gleaned from the micrograph in Fig. 1, where a cross section of the oxidized wire is illustrated. The IrO_x growing from the Ir wire exhibits a columnar structure with high aspect ratio grains. The small cracks between the Ir metal and the IROF are believed to result from the preparation process for the SEM sample, as the cross section of Ir wire was sand papered. The thick IROF is strongly adherent to the Ir substrate and hard to scrape off, in contrast to AIROF which is usually poorly adherent and easily removed from the substrate due to its highly hydrated nature.[10] The IROF prepared by thermal decomposition of $IrCl_3$ on a Ti substrate is also poorly adherent as it tends to be powdery.[30,34] In addition, IROFs prepared by thermal and electrochemical growth methods show extensive cracking and poor mechanical stability.[26,37,38] Stability in strong acid/base solutions is a key property of an IROF for a pH electrode. It is found that the current IROF is very stable both in strong acid and strong alkaline solutions, and even withstands sonication in a 4 M HCl solution for 24 h. AIROF, on the contrary, can be completely dissolved from the electrode surface by soaking in 5 M hot H_2SO_4[33] or in 12 M hot HCl with a few drops of H_2O_2.[37] Neither of these two solutions attacks the IROF prepared by the present method. Clearly, with its high chemical stability in strong acid/base and oxidizing solutions, the present IROF may also find its application as a stable anode material for O_2 and Cl_2 evolutions. Another special property of the present IROF is its color. The present IROF is deep black, quite different from the dark blue IROFs prepared by other methods (see Table I). The possible reason for this phenomenon is the involvement of Li^+ in the IROF prepared. Reportedly the chemical insertion of Li^+ in NiO results in a color change from light green to black.[39]

The thickness and morphology of the oxide film were found to be dependent on the oxidation temperature, time duration, atmosphere, and the kind of carbonate used. Under the present condition, *i.e.*, oxidation at 870°C for 5 h in Li_2CO_3 melt under air atmosphere, the thickness of the IROF is about 20 μm, as shown in Fig. 1.

Composition of the IROF.—The oxide powder scraped from oxidized wires was collected for characterization. Elemental analysis results obtained from ICP-OES and ICP-MS indicate that the IROF contains about 77 wt % Ir and 2.4 wt % Li, corresponding to 1:0.86 in atomic ratio of those two elements. The large amount of Li comes from the Li_2CO_3 melt in which the oxide film was produced. XPS results indicate that the IROF is highly hydrated due to the treatment of the film with HCl solution in the fabrication process. It is observed that the extent of hydration can be held almost constant even after the oxide is heated at 200°C overnight. Here we use the formula of $Li_xIrO_y \cdot nH_2O$ to present the oxide layer, chiefly IrO_x in this paper, although more information is needed to formulate the oxide compound exactly. More detailed composition analysis is underway.

XPS spectra were taken for the prepared IrO_x and for commercial IrO_2 powder as a reference. The O 1s and $Ir_{4f7/2,5/2}$ XPS spectra for the two samples are presented in Fig. 2. In (a) and (b), the O 1s signals were deconvoluted into three peaks, corresponding to three different oxygen species, *i.e.*, undissociated water, OH groups, and lattice oxide.[40] The relative abundance of these oxygen species can be estimated from the deconvoluted peak area. For commercial IrO_2, the contribution from H_2O is small, indicating that the powder is almost unhydrated. While for IrO_x, the most important oxygen species is H_2O, indicating that the IrO_x is highly hydrated. It is believed that a stable hydration state is important for pH sensing in the present IrO_x electrode. It is noted that although the present IrO_x is highly hydrated, it is different from the hydrated IROF made from electrochemical growth method. For example, the latter commonly shows super-Nernstian behavior, while the present electrode always exhibits near Nernstian slope as discussed later.

XPS results of IrO_x and commercial IrO_2 powder for Ir $4f_{7/2}$ and $4f_{5/2}$ are illustrated in Fig. 2c and d. The electron binding energies of $Ir4f_{7/2}$ and $4f_{5/2}$ were 62.1 and 65.1 eV for IrO_2, and 63.1 and 65.8 eV for IrO_x powder, respectively. The higher binding energy indicates that the IrO_x sample probably has a higher oxidation state than 4, which is the most common oxidation state of Ir in oxides.

Formation mechanism of IROF.—An understanding of the mechanism of metal oxide film growth in carbonate melts is important from both the fundamental and practical perspectives. It may help the understanding of the composition and electrochemical properties of the IROF, and consequently, the optimization of the fabrication condition, to produce better pH electrodes. Since Ir is a noble metal belonging to the platinum family, so preparation of IROF by oxidation of an Ir metal is not easy. The present method to make IROFs is a novel although basically a thermal technique. The present method, *i.e.*, the carbonate melt method, is different in many aspects compared to the nitrate melt method reported in literature.

First, the oxidizing species are different for the two methods. In a nitrate melt, the oxidant is KNO_3, while in a carbonate melt it is O_2^{2-}, which is produced from the reaction of dissolved O_2 in the melt with CO_3^{2-}. Actually, if the carbonate melt is not exposed to an atmosphere containing O_2, it will lose its oxidizing ability toward metals. We found that in an air atmosphere, Ir wire can be oxidized in Li_2CO_3 melt and a thick oxide layer grows on the surface of the wire within 1/2 h. While Li_2CO_3 melt is exposed to a N_2 atmosphere, even after 24 h there is no visible oxide layer grown on the metal surface, which implies that access to oxygen is necessary for the oxidation process.

The reaction medium in the two methods provides different acid-base environment. In an alkali metal carbonate melt (A_2CO_3, A=alkali metal), the following equilibria exist

$$A_2CO_3(l) = 2A^+ + CO_3^{2-} \quad [1]$$

$$CO_3^{2-} = O^{2-} + CO_2(g) \quad [2]$$

where the CO_3^{2-} and O^{2-} contribute to the alkalinity of the melt while the CO_2 is the acidic component. Alkali metal carbonate melt exhibits a strong alkaline behavior in air atmosphere, while a nitrate melt is nearly neutral.

As for the oxidation temperature, its value is mainly limited to the temperature range between the melting point and the decomposition temperature of the salt used. The temperature for the carbonate melt method is much higher than that for the nitrate melt method. We believe that both the acid-base property of the medium and the temperature are crucial for the formation of the metal oxide film. The reason is that the two factors can greatly affect the composition and the solubility of the produced oxide in the melt. The solubility determines whether the oxide film is deposited on the metal substrate or dissolved in the melt.

The stronger oxidation power of a carbonate melt over that of a nitrate melt make the former more favorable to oxidize metals. For example, in a nitrate melt, oxidation of metals such as Nb, Pd, Ta, etc., can only happen with an externally applied potential.[41] In this case, the preparation process is more like an electrochemical oxidation. On the other hand, a carbonate melt can oxidize most metals including Ni, Pt, Ag, Cu and Fe without bias assist.[42-45]

Carbonate melt is well known as the electrolyte in molten carbonate fuel cells (MCFC). The corrosion behavior of Ni metal in a carbonate melt,[44] mostly in an eutectic $(Li_{0.62}K_{0.38})_2CO_3$ mixture, has been investigated extensively to improve the performance and lifetime of Ni cathodes in MCFC. It has been proposed that the oxidation mechanism of a metal in a carbonate melt involves the formation of a peroxide ion (O_2^{2-}).[45] In this process O_2 from the atmosphere dissolves in the melt and reacts with carbonate ions to form O_2^{2-}, which is a strong oxidizer especially at high temperature. O_2^{2-} oxidizes the metal and gets reduced to O^{2-}

$$O_2(\text{dissolved}) + 2CO_3^{2-} = 2\,O_2^{2-} + 2CO_2 \quad [3]$$

$$O_2^{2-} + 2e^- = 2\,O^{2-} \quad [4]$$

while the metal M is being oxidized

$$M = M^{2+} + ze^- \quad [5]$$

Here, z is the valence of metal M. Hence, the overall reaction is the oxidation of the metal by O_2^{2-} is

$$2/zM + O_2^{2-} = M_{2/z}O + O^{2-} \quad [6]$$

Obviously, the solubility of the produced metal oxide in the carbonate melt is critical for the formation of the above oxide film on the metal surface. If the metal oxide is soluble, as in the case of Cr_2O_3 where soluble chromate forms, the melt will dissolve the oxide without precipitation of an oxide layer.[46] On the other hand, if the oxide is insoluble, a stable oxide layer may form as in the current case, where an iridium oxide layer grows on the Ir surface.

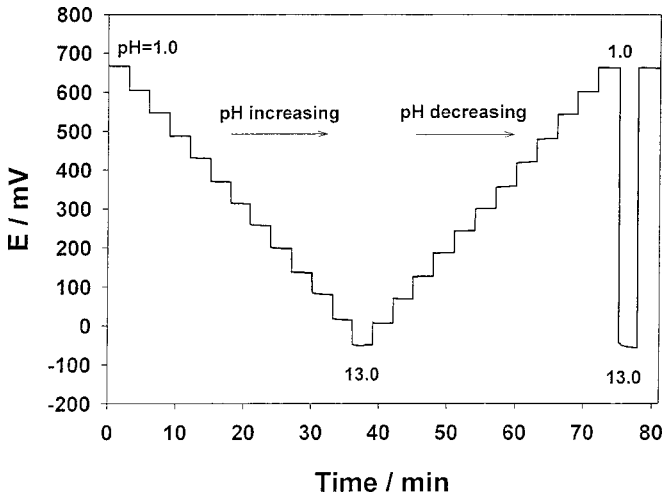

Figure 3. Potential response of an IrO_x electrode (batch I) to pH changes in a series of pH buffer solutions from pH 1 to 13.

For some metal oxides produced in a Li_2CO_3 melt, lithiation may occur and a Li-containing product is formed[44,45]

$$M_{2/z}O + Li_2O \rightarrow Li_xMO_y \quad [7]$$

When the produced oxide compound is treated in an acid solution, a hydration process takes place

$$Li_xMO_y + nH_2O \rightarrow Li_xMO_y \cdot nH_2O \quad [8]$$

The properties of the metal oxide can be greatly affected by the insertion of lithium ions. For example, the lithiation of NiO electrode in Li_2CO_3 melt produces Li_xNiO_y, which can enhance the electronic conductivity and lifetime of the NiO electrode for MCFC application.[44] In our case, the lithiation of iridium oxide seems to contribute much to the chemical stability of the IROF and to the pH sensing performance of the electrode. Of course, further research is needed to investigate whether other combinations of carbonate salts and metals can also produce pH electrodes with good performance.

pH response.—The IrO_x electrodes made by the described method were evaluated in pH buffer solutions. Figure 3 shows a typical OCP response of an IrO_x electrode to step pH changes of one unit between pH 1 and 13. The pH changes were realized by method I, *i.e.*, by changing fresh commercial pH buffer solutions. The calibration of the electrode was carried out in both directions, *i.e.*, from pH 1 to 13 and vice versa. It is apparent from Fig. 2 that the electrode provides excellent reversibility, independent of pH value and the direction of pH change. Even when the pH was changed cyclically in large steps, as between pH 1 and 13, the potential response shows very good reversibility and almost no hysteresis.

Long-term stability of slope and $E^{\circ\prime}$.—From a practical point of view, long-term stability is an important feature of a sensor. Six separate runs were performed using the same IrO_x electrode over 100 days for long-term stability test in commercial pH buffer solutions (method I). As manifested in Fig. 4, the calibration curves show very good linearity and the potential response of the electrode was very stable over such a long test period. The average variation of the $E^{\circ\prime}$ values for the six tests is less than 5 mV during the 100 day test period, with no specific direction of potential variation. Over this long period, temperature variations due to day-to-day room temperature changes may explain the $E^{\circ\prime}$ changes. After this period of use, including exposure to various pH buffer solutions, being stored in a 4 M KCl solution or in air, there is not any change

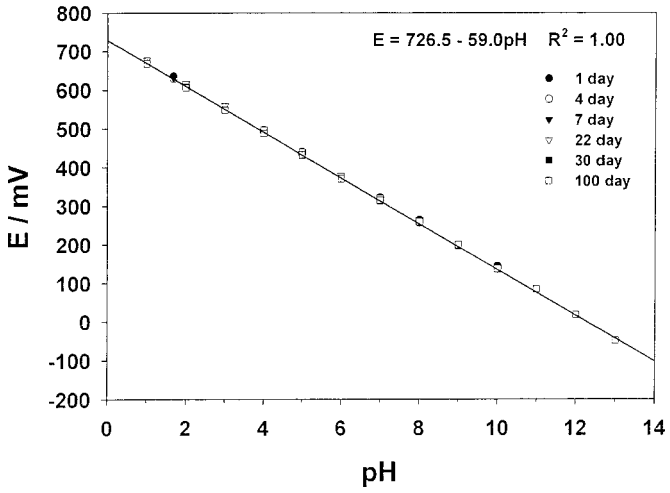

Figure 4. Long-term stability of the IrO_x pH electrode (batch I) in pH buffer solutions. Between the tests, the pH electrode was stored in air, in a pH buffer, or in a 4 M KCl solution.

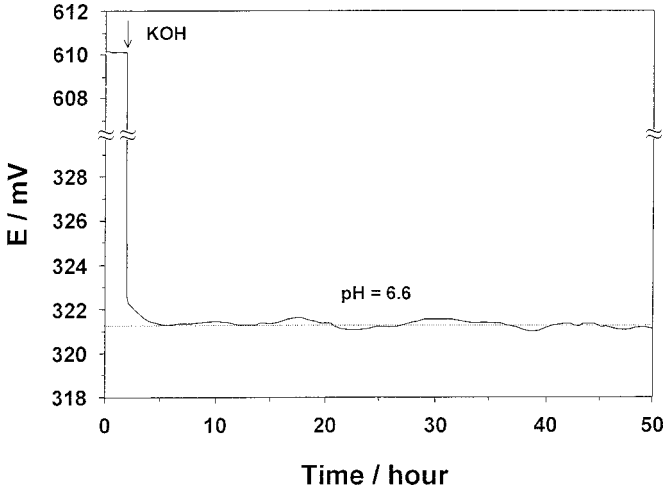

Figure 5. Potential stability of an IrO_x electrode (batch II) in a pH 6.6 buffer solution. The test is performed in an unthermostated measurement cell at room temperature after a pH change from pH 1.8 to 6.6 by KOH titration.

in pH sensitivity, *i.e.*, the slope always remains near ~59 mV/pH. Obviously, the present electrode, unlike a glass electrode, does not require special care. The stable linear potential response implies that a two-point calibration, as usually made with a glass electrode, would be sufficient for the current IrO_xpH electrode. It is worth mentioning that data presented here were obtained without previous conditioning of the electrode, *i.e.*, no aging effects were observed, which is probably due to the stable hydration state of the IrO_x film. It is suggested that aging effect of an electrode be attributed to a hydration degree change of the oxide layer. In our case, the IrO_x layer retains almost the same hydration state, all the time irrespective, if the electrode was stored in air or in solution. These results prove that the IROF prepared by the present novel method is highly stable for long-term applications.

The linear potential response also suggests that various anions contained in commercial pH buffer solutions, such as phosphate, acetate, citrate, borate, chloride, nitrate, carbonate, etc., do not affect the pH response of the IrO_x electrode. Neither do the tested alkaline cations like Li^+, K^+, Na^+, and Ca^{2+}. Usually redox interference is a serious problem with metal oxide electrodes, as discussed in the introduction. As we found, the electrodes suffer some interference from strong reducing species, such as ascorbic acid, but not from oxidizing agents such as Fe^{3+}, ferricyanide, and oxygen. It is also observed that the electrode does not show measurable interference from stirring of the solution or dissolved oxygen, similar to the results reported previously.[10,25] Detailed investigation on redox interference, including optimization of the preparation condition of the electrode or coating a polymer membrane to minimize the effect of reducing agents is in progress.

Stability of OCP.—In the previous section, it is shown that the electrode exhibits good long-term stability over a period of 100 days. However the measurements were carried out only several times during this period. In this section, a continuous test in a solution to identify potential drift with time is presented. Potential drift in a continuous test will cause error in pH measurements, and it can not be eliminated by calibration. The drift behavior of the present IrO_x electrodes was evaluated in a pH buffer solution stirred under air at room temperature. Figure 5 shows the potential change with time of an IrO_x electrode in a pH 6.6 buffer solution. The value of the potential is almost constant at 321.2 mV with a deviation of less than ± 0.2 mV over a period of two days. It is most likely that this small deviation results from variation in room temperature because the potentials of the IrO_x electrode and Ag/AgCl reference electrode and the actual pH of the solution are all temperature dependent, as the test solution is not thermostated. The potential drift, *i.e.*, potential change with time in a specific direction, cannot be established from the present test. In Fig. 5, the pH electrode was first exposed to a pH 1.8 solution and then added KOH to increase the pH to 6.6. We see from the figure that the electrode quickly responded to this pH change and established a new equilibrium potential. High stability of the present IrO_xpH electrode makes it suitable for continuous measurements without the need for frequent calibration.

Reproducibility.—An indication of the electrode reproducibility can be obtained by measuring a group of electrodes made from the same batch. In the measurements, all the electrodes were put in the same buffer solution sharing the same reference electrode to ensure an identical condition for all the electrodes. In the present experiment, 12 pieces of IrO_x electrodes from the same batch were used, which are a sufficiently large number for statistical analysis of the test result. Figure 6 shows the pH response transients of the 12 electrodes during a titration of the base pH buffer with KOH

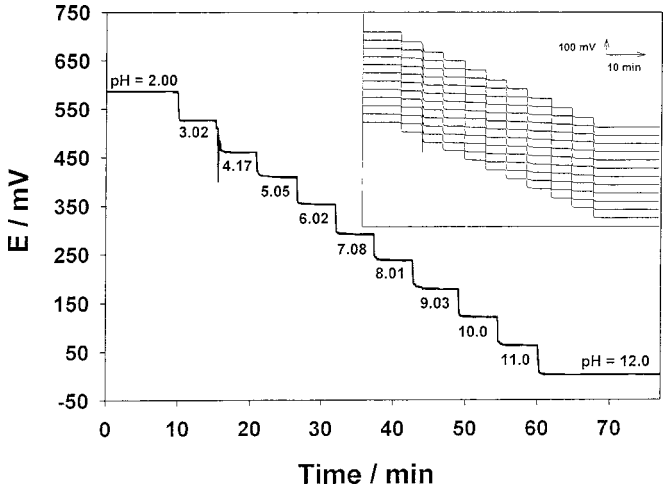

Figure 6. Dynamic response transients for 12 IrO_x electrodes (batch II) from the same batch. The pH changes were realized by additions of 1 M KOH solution to a universal buffer solution. The pH values indicated in the figure were measured with a glass electrode. For more detailed comparison, the potential curves for different pH electrodes were taken apart from each other as shown in the inset.

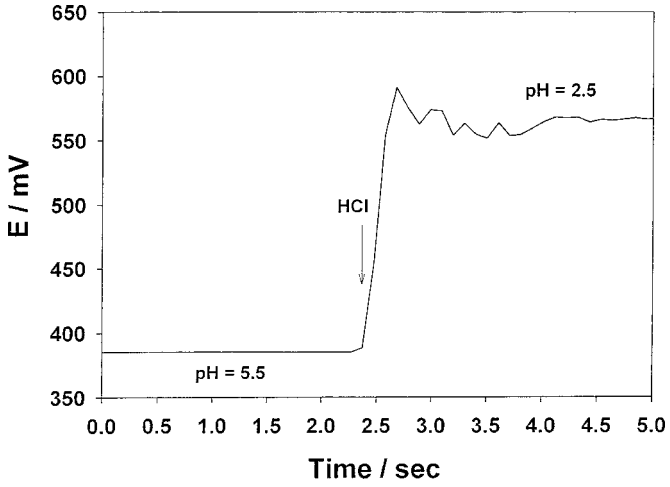

Figure 7. Potential-response time curve of the IrO_x electrode (batch II). The pH change from pH 5.5 to 2.5 is realized by a sudden addition of HCl to a buffer solution. The 90% response time is less than 0.2 s.

(method II). The pH values of the buffer solution, indicated in the figure, were measured with a glass electrode. The response transients for all of the 12 electrodes are overlapped perfectly, demonstrating excellent reproducibility. For a detailed comparison of these electrodes, the response curves are purposely separated from one another as shown in the inset. The potential response curves to stepwise pH increases from 2 to 12 at intervals of about one pH are basically identical for all of the 12 electrodes. They exhibit very similar response times and potential response with pH changes. The standard deviation of slopes is as small as ± 0.1 mV/pH, and $E^{\circ\prime}$ is ± 0.3 mV. Such excellent reproducibility both in slope and $E^{\circ\prime}$ has not been reported in the literature. For example, for a batch of thermally oxidized IrO_x electrodes, Hitchman *et al.*[28] observed that the variation in $E^{\circ\prime}$ could be more than 100 mV, and Kinlen *et al.*[30] reported that the standard deviation for slopes was 6.2 mV/pH. From the viewpoint of practical applications, the very close agreement with respect to Nernstian slopes and $E^{\circ\prime}$ values among different IrO_x electrodes prepared by the present method represents a significant advantage over glass electrodes, which are known to have large variations in $E^{\circ\prime}$. However, the $E^{\circ\prime}$ values vary for different batches of IrO_x electrodes, indicating that more careful control of the fabrication condition is needed.

Response time.—In order to evaluate the response time of the IrO_x electrodes, a rapid step change in pH was realized by quickly adding a certain amount of HCl solution into the test solution with a syringe. During the experiment the test solution was stirred vigorously. A typical dynamic response curve is presented in Fig. 7. In the figure, a fast response with a damped oscillation in the potential reading is observed on adding HCl solution. The damped oscillation results from the solution mixing, *i.e.*, it takes several seconds for the solution to get a uniform pH value. The time for the electrode potential to reach a stable equilibrium value was very short. The response time, defined as 90% of the full response, was about 0.2 s for the step change from pH 5.5 to 2.5. The response time of the present electrode was much shorter than that of other IrO_x electrodes reported previously. Reported data on response time usually range from a few seconds to a few minutes.[25,27,30] It is noted that the real response time of the present electrode probably is <0.2 s as it is limited by solution mixing. It was observed that the response time was influenced by the solution volume and the stirring speed. By special design of the measurement setup, the response time could be determined more accurately.

Sensing mechanism.—The pH sensing mechanisms for AIROF based electrodes are not confirmed yet, although some possible mechanisms have been proposed on the basis of pH dependent redox equilibrium between two oxidation states of the iridium oxide. The most feasible one is considered to be[27,28]

$$2IrO_2 + 2H^+ + 2e^- = Ir_2O_3 + H_2O \qquad [9]$$

$$E = E^\circ - 2.303RT/F \ \text{pH}$$
$$= E^\circ - 59.16 \ \text{pH} \qquad [10]$$

where E° is the standard electrode potential with the value of 926 mV (*vs.* SHE),[47] and RT/F has its usual meaning. The potential/pH slope is expected to be $\sim$59.16 mV/pH at 25°C.

From Fig. 4, a near ideal Nernstian slope of 59 mV/pH is observed experimentally. The intercept at pH 0 gives an $E^{\circ\prime}$ value of 726.3 mV *vs.* Ag/AgCl reference electrode, or 923.3 mV *vs.* standard hydrogen electrode (SHE), which is very close to the theoretical value associated with Reaction 9.

It is found that the IrO_x electrodes made from the same batch can give very close $E^{\circ\prime}$ values, however for different batches the electrode show different $E^{\circ\prime}$ values. We believe that the variation of $E^{\circ\prime}$ for different batches may result from the variation in the stoichiometry of the oxide compound, and consequently the difference of its oxidation state. An oxygen intercalation mechanism,[7] in which an iridium oxide couple (higher and lower valence) get equilibrium, is believed to better describe the sensing mechanism of the present electrode

$$Li_xIrO_y + 2\delta H^+ + 2\delta e^- \rightarrow Li_xIrO_{y-\delta} + \delta H_2O \qquad [11]$$

where Li_xIrO_y (the water of hydration omitted) has a higher oxidation state and $Li_xIrO_{y-\delta}$ is an oxygen deficient phase with a lower oxidation state. Following a similar treatment reported previously,[28] the equilibrium potential can be represented by

$$E = E^\circ + \frac{2.303RT}{2\delta F} \log\frac{[Li_xIrO_y][H^+]^{2\delta}}{[Li_xIrO_{y-\delta}]}$$
$$= E^\circ + \frac{2.303RT}{2\delta F} \log\frac{[Li_xIrO_y]}{[Li_xIrO_{y-\delta}]} + \frac{2.303RT}{F} \log[H^+]$$
$$= E^{\circ\prime} - \frac{2.303RT}{F} \ \text{pH}$$
$$= E^{\circ\prime} - 59.16 \ \text{pH} \qquad [12]$$

From Eq. 12, the $E^{\circ\prime}$ depends on the ratio of $[Li_xIrO_y]/[Li_xIrO_{y-\delta}]$, *i.e.*, the higher the ratio, the higher the $E^{\circ\prime}$ value. The ratio of the two species in turn, is related to the oxidation state of the IROF. As discussed in a previous section the carbonate melt used in the present work provides strong oxidizing condition, under which a higher oxidation state of IROF will be produced. Therefore a higher $E^{\circ\prime}$ value will be expected. Indeed, in our experiments, most of the observed $E^{\circ\prime}$ values are higher than the E° from Eq. 10, *i.e.*, 926 mV *vs.* SHE. As stated above, the molten carbonate oxidation produces a nonstoichiometric compound; therefore it is difficult to control the oxidation state of Ir. If this is taken into account, it seems understandable that there exists a variation in $E^{\circ\prime}$ values for electrodes from different batches.

Conclusions

This paper has described a new fabrication methodology for IrO_x-based pH electrodes. The IROF made by an oxidation of an Ir metal in a Li_2CO_3 melt has the composition of $Li_xIrO_y \cdot nH_2O$. The IrO_x pH electrode prepared this way is characterized by ideal Nernstian response (58.92 mV/pH) over a wide pH range, fast response (<0.2 s), almost drift-free (<0.1 mV/day), and excellent reproducibility of the electrode. The electrode described here is of great

promise for pH sensing and could, in many applications, replace glass electrodes or other metal oxide-based electrodes.

The Ohio State University assisted in meeting the publication costs of this article.

References

1. H. Galster, *pH measurements-Fundamentals, Methods, Applications, Instruments*, VCH Publishers, New York (1991).
2. M. J. Madou and S. R. Morrison, *Chemical Sensing with Solid State Devices*, Academic Press, New York (1989).
3. D. J. G. Ives and G. J. Janz, *Reference Electrodes*, Academic Press, New York (1961).
4. R. E. F. Einerhand, W. H. M. Visscher, and E. Barendrecht, *Electrochim. Acta*, **34**, 345 (1989).
5. C. C. Liu, B. C. Bocchicchio, P. A. Overmyer, and M. R. Neuman, *Science*, **207**, 188 (1980).
6. W. T. Grubb and L. H. King, *Anal. Chem.*, **52**, 270 (1980).
7. A. Fog and R. P. Buck, *Sens. Actuators*, **5**, 137 (1984).
8. K. Pásztor, A. Sekiguchi, N. Shimo, N. Kitamura, and H. Masuhara, *Sens. Actuators*, **B13-14**, 561 (1993).
9. H. N. McMurray, P. Douglas, and D. Abbot, *Sens. Actuators*, **B28**, 9 (1995).
10. L. D. Burke, J. K. Mulcahy, and D. P. Whelan, *J. Electroanal. Chem.*, **163**, 117 (1984).
11. E. Kinoshita, F. Ingman, G. Edwall, S. Thulin, and S. Glab, *Talanta*, **33**, 125 (1986).
12. M. L. Hitchman and S. Ramanathan, *Analyst (Cambridge, U.K.)*, **113**, 35 (1988).
13. W. Olthuis, M. A. M. Robben, P. Bergveld, M. Bos, and W. C. Van Der Linden, *Sens. Actuators*, **B2**, 247 (1990).
14. I. Song, K. Fink, and J. H. Payer, *Corrosion (Houston)*, **54**, 13 (1998).
15. R. K. Jaworski and J. A. Cox, *J. Electroanal. Chem.*, **325**, 111 (1992).
16. J. E. Baur and T. W. Spaine, *J. Electroanal. Chem.*, **443**, 208 (1998).
17. S. A. M. Marzouk, S. Ufer, R. P. Buck, T. A. Johnson, L. A. Dunlap, and W. E. Cascio, *Anal. Chem.*, **70**, 5054 (1998).
18. T. Katsube, I. Lauks, and J. N. Zemel, *Sens. Actuators*, **2**, 399 (1982).
19. I. Lauks, M. F. Yuen, and T. Dietz, *Sens. Actuators*, **4**, 375 (1983).
20. M. J. Tarlov, S. Semancik, and K. G. Kreider, *Sens. Actuators*, **B1**, 293 (1990).
21. A. Kato, Y. Konno, Y. Yanagida, M. Yamasato, T. Taguchi, R. Motohashi, and T. Katsube, *Anal. Sci.*, **7**, (suppl) 1577 (1991).
22. K. Izutsu and H. Yananoto, *Anal. Sci.*, **12**, 905 (1996).
23. K. G. Kreider, M. J. Tarlov, and J. P. Cline, *Sens. Actuators*, **B28**, 167 (1995).
24. J. V. Dobson, P. R. Snodin, and H. R. Thirsk, *Electrochim. Acta*, **21**, 527 (1976).
25. G. Papeschi, S. Bordi, C. Beni, and L. Ventura, *Biochim. Biophys. Acta*, **453**, 192 (1976).
26. S. Ardizzone, A. Carugati, and S. Trasatti, *J. Electroanal. Chem.*, **126**, 287 (1981).
27. K. Kinoshita and M. J. Madou, *J. Electrochem. Soc.*, **131**, 1089 (1984).
28. M. L. Hitchman and S. Ramanathan, *Talanta*, **39**, 137 (1992).
29. M. L. Hitchman and S. Ramanathan, *Analyst (Cambridge, U.K.)*, **116**, 1131 (1991).
30. P. J. Kinlen, J. E. Heider, and D. E. Hubbard, *Sens. Actuators*, **B22**, 13 (1994).
31. M. Ue and J. F. Coetzee, *Denki Kagaku oyobi Kogyo Butsuri Kagaku*, **65**, 401 (1997).
32. S. Trasatti, *Electrochim. Acta*, **36**, 225 (1991).
33. S. Gottesfeld and J. D. E. McIntyre, *J. Electrochem. Soc.*, **126**, 742 (1979).
34. L. D. Burke and D. P. Whelan, *J. Electroanal. Chem.*, **162**, 121 (1984).
35. M. J. Madou, *Fundamentals of Microfabrication*, CRC Press, New York (1997).
36. N. Bestaoui, E. Prouzet, P. Ceniard, and R. Brec, *Thin Solid Films*, **235**, 35 (1993).
37. P. G. Pickup and V. I. Birss, *J. Electrochem. Soc.*, **135**, 126 (1988).
38. B. E. Conway and J. Mozota, *Electrochim. Acta*, **28**, 9 (1983).
39. P. Tomczyk, H. Sato, K. Yamada, T. Nishina, and I. Uchida, *J. Electroanal. Chem.*, **391**, 125 (1995).
40. R. Sanjines, A. Aruchamy, and F. Levy, *J. Electrochem. Soc.*, **136**, 1740 (1989).
41. R. L. Every, *J. Electrochem. Soc.*, **112**, 524 (1965).
42. G. J. Janz, A. Conte, and E. Neuenschwander, *Corrosion (Houston)*, **19**, 292 (1963).
43. P. Claes, B. Thirion, and J. Glibert, *J. Electroanal. Chem.*, **389**, 37 (1995).
44. B. Malinowska, M. Cassir, F. Delcorso, and J. Devynck, *J. Electroanal. Chem.*, **21**, 389 (1995).
45. M. Spiegel, P. Biedenkopf, and H. J. Grabke, *Corros. Sci.*, **39**, 1193 (1997).
46. C. G. Joo, C. W. Yi, C. Kang, and K. Kim, *J. Power Sources*, **72**, 211 (1998).
47. M. Pourbaix, *Atlas of Electrochemical Equilibria in Aqueous Solutions*, p. 374, Pergamon Press, Oxford, U.K. (1966).